Proceedings of the 15th
IEEE International Conference on Nanotechnology
July 27-30, 2015, Rome, Italy

Effects of Impurities and Lattice Imperfections on the Conductive Properties of MoS_2*

Andrew Stroud and Pedro A Derosa
Institute for Micromanufacturing and Dept. of Physics
Louisiana Tech University
Ruston, LA, USA

Christopher Muratory
Dept. of Chemical and Materials Engineering
University of Dayton
Dayton, OH, USA

Gary Leuty, Christopher Muratore and Rajiv Berry
Materials and Manufacturing Directory
Air Force Research Lab
Dayton, OH USA

Pedro A Derosa
Dept. of Mathematics and Physics
Grambling State University
Grambling, LA, USA

***Abstract* — The effects of vacancies on the electronic properties of transition metal dichalcogenide (TMD) semiconductors is studied and the absorption of water demonstrated by modeling molybdenum disulfide (MoS_2) nanoscale devices. The simulations presented here combine molecular dynamics (MD), density functional theory (DFT), and non-equilibrium Green's function (NEGF) formalism. Combining these methods, the effects of single and double S vacancy and a single Mo vacancy on charge transport are detailed by looking at transmission functions and conduction paths. The contrast on the effect of double S vacancy and Mo vacancy is intriguing, with only hole transport and electron transport respectively, being affected by the defect. Adsorption of water and oxygen at defects, particularly grain boundaries, is demonstrated via MD simulations.**

Keywords—Modeling, 2-D Materials Beyond Graphene, Device

I. Introduction

TMDs have garnered widespread attention as the next step in 2D materials after the semi-metal graphene. Current applications of these materials include solar cells, batteries, superconductors, and field effect transistors [1]. Single layers of TMDs such as MoS_2, $MoSe_2$, WS_2 and WSe_2 have been shown to have direct bandgaps within the range of 1.5 to 2.0 eV [2]. Experimental device creation rarely results in perfect crystals and humidity is detrimental to device performance [3]. Grain boundaries and the presence of adsorbents can cause considerable alterations in the electronic properties of these materials, leading to reduced conductivity [3]; however, grain boundaries in MoS_2 monolayers can also incorporate metallic and magnetic properties into the semiconductor [4]. Similarly, exposed Mo atoms in MoS_2 have been shown to become oxidation and dissociation sites for various molecular species, including water [5], which is of great relevance as MoS_2 has become a material of interest for applications such as water splitting [6] and Hydrogen Evolution Reaction [7]. The thermal properties of TMD materials have previously been studied using classical molecular dynamics (MD) simulations [8], but electronic and transport properties still need careful study.

*Research supported by Air Force RCP contract FA8650-13-C-5800 from the AFRL Materials & Manufacturing Directorate, WPAFB, OH. Ms. Asheley Blackford, Program Manager. Computer resources provided by Louisiana Optical Network Initiative (LONI) and the DoD Supercomputer Center.

II. Methodology

The Atomistix ToolKit [9] computational software suite was used to study properties of MoS_2 devices consisting of two electrodes and a central scattering region all made of MoS_2 as shown in Fig. 1. The device is periodic in the directions transverse to the current (x, y), while the electrodes are created by copying a portion of the central scattering region along z. Metal electrodes should instead by modelled if an actual device is to be simulated; however, by having MoS_2 as the electrode material as well, the observed behavior can be undoubtedly attributed to MoS_2 properties without the effect of a junction.

The current through the central region of the device is calculated for a given voltage by using the Landauer-Büttiker formalism:[10]

$$I(V) = \frac{2e}{h}\int_{\mu_L}^{\mu_R}\big(f(E-\mu_L) - f(E-\mu_R)\big)T(E)dE$$

Here μ_L and μ_R are the chemical potentials for the left and right electrodes, respectively, $f(E-\mu)$ is the Fermi-Dirac distribution function, and $T(E)$ is the transmission function, which is obtained from the Green's function of the central region, in turn obtained from DFT. Further device transport properties analyzed include: density of states, electron density, molecular orbitals, transmission pathways, vibrational modes, and optical properties [9].

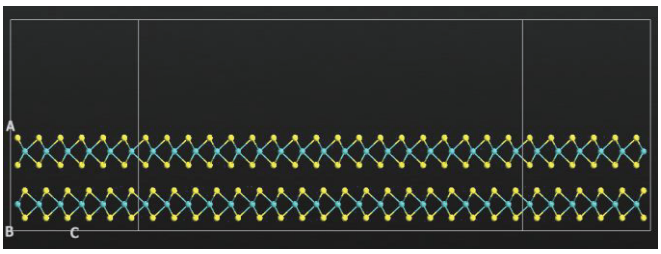

Fig. 1: Side view of a bilayer MoS_2 device

III. Results

A. S and Mo Vacancies

A 4x4 supercell of bilayer MoS_2 consisting of 95 atoms was used to study the effects of surface vacancies on the

bandstructure. The surface vacancies being studied consisted of a single or two missing S atoms or a missing Mo atom in the top layer of MoS_2. Next, these vacancies were placed into a device configuration 5 nm long, as shown in Fig. 1, and the densities of states (DOS), transmission functions (TF), and conduction paths were obtained.

An indirect band gap of 1.24 eV for the pristine bilayer system is shown in Fig. 2a. With the introduction of each vacancy, mid-gap bands are formed between the conduction and valence bands of the pristine bilayer MoS_2 (Figs. 2b-d). These mid-gap bands create scattering centers within the material and correspond to the opening of orbitals in the density of states. These effects are similar to those that have been extensively studied in monolayer MoS_2 systems [11].

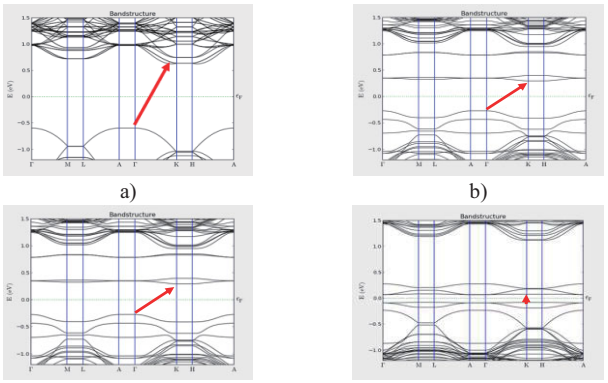

Fig. 2: Bandstructure of bilayer MoS_2 for: a) pristine bilayer (band gap 1.24eV); b) single S atom vacancy (band gap 0.69eV); c) S pair vacancies (band gap 0.56); and d) single Mo atom vacancy (band gap 0.16eV). The band gaps in each case are indicated by the red arrows.

The device DOS and TF are shown in Fig. 3. The logarithmic scale clearly shows the mid-gap states produced by the defects.

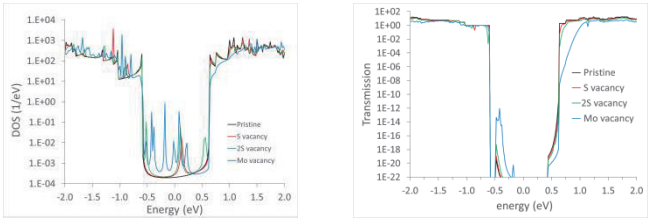

Fig. 3: a) Density of states and b) transmission function of the bilayer device in Fig. 1, for pristine bilayer and defective top layers.

Fig. 4 shows the current vs. voltage for each of the four cases. The electrode regions were artificially *p* and *n* doped to change the electrostatic potential of the electrodes, thus allowing the study of regions of higher conductivity at a lower voltage, making the calculations more efficient. The effect of gap states is very clearly evidenced by the larger current for defective devices. Figs. 4b and 4c show the electronic structure of a p-i-n device, where a set of gap states is observed around the Fermi level (Fig. 4c) for a Mo vacancy.

For negative biases, the depletion zone decreases activating the gap states shown in Fig. 4c what leads to a larger current in the Mo-vacant device. At larger voltages, conductivity occurs through main channels and the pristine device outperforms the defective ones.

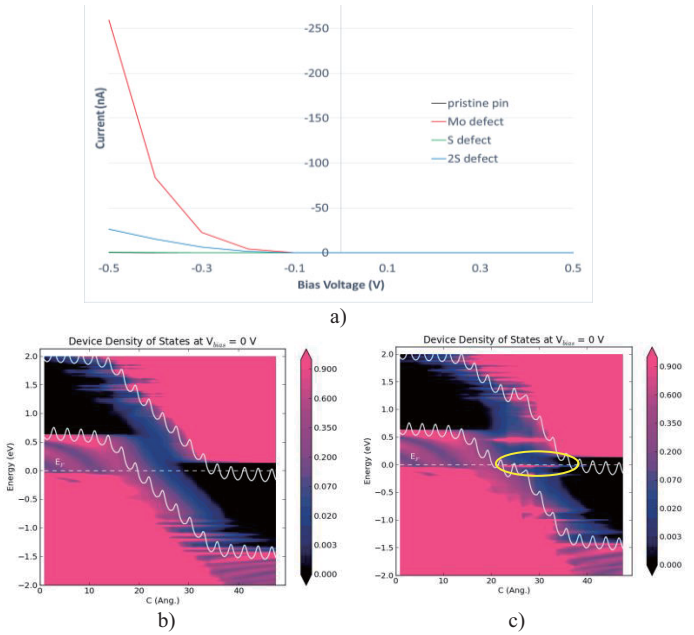

Fig. 4: (a) Current vs. voltage through a bilayer MoS_2 device with and without vacancies. For these calculations, the electrodes were *p* and *n* doped to change their electrostatic potentials. Device DOS (color coded from black to pink) for (b) pristine and (c) Mo-vacant cases show the effect of electrode doping. Conduction is through the gap, so gap states (see yellow contour) are responsible for the larger conductivity of Mo-vacant seen in the I-V curves.

Figs. 5 and 6 show respectively the conduction paths for electrons and holes at the edge of the band gap, the paths the electrons and holes will use to conduct when the voltage is large enough to reach the conduction and valence bands.

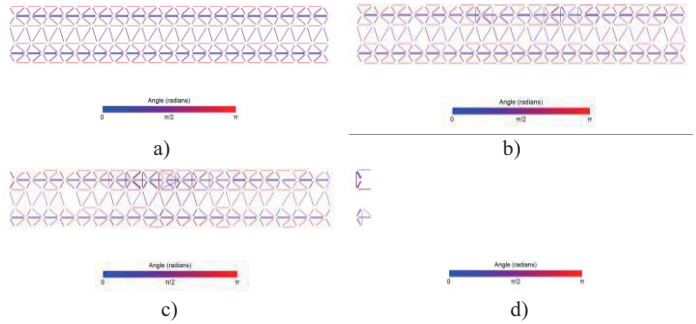

Fig. 5: Conduction paths for electrons in a) pristine; b) single S vacancy; c) double S vacancy; and d) Mo vacancy. The colors blue or red indicate the phase.

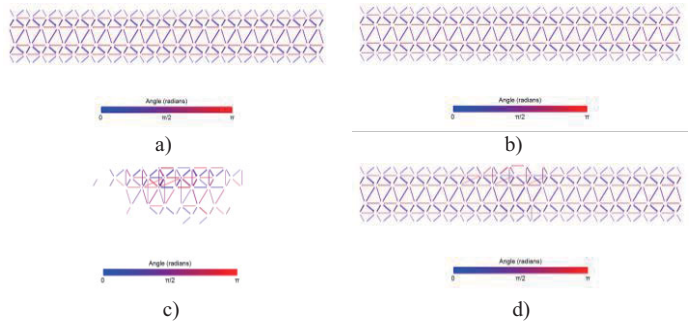

Fig. 6: Hole conduction paths for a) pristine; b) single S vacancy; c) double S vacancy; and d) Mo vacancy. The colors blue or red indicate the phase.

Electron conduction occurs mainly as an intralayer process for the pristine device with some weak interlayer transport. The removal of one or two S atoms from the top layer only marginally disrupts electron transport, with a higher effect in the double vacancy case. However, for Mo vacancy, the electron transport is completely suppressed, both inter- and intralayer.

For hole transport, the behavior is somewhat different in the pristine case as hole transport is observed to be strong both within and between layers. A single S vacancy does not seem to alter hole transport very much, while a double S vacancy creates a trap in the region of the vacancy suppressing any conductivity between the device and the electrodes. For the case of a Mo vacancy, some scattering arises in the defect area, but hole conductivity is not greatly disturbed.

The result is quite intriguing, while double S vacancy completely suppresses hole transport barely affecting electron transport. The opposite behavior is observed for a Mo-vacancy.

B. Water and Oxygen Impurities

The existence of vacancies and grain boundaries (not studied here) create sites where moisture in the environment, as well as oxygen, can be absorbed. In this part of the study, the absorption of these two species is studied.

A 6x6 supercell of bilayer MoS_2 is used to examine the absorption of water at a grain boundary and at edges (Fig. 7) and edge oxidation (Fig. 8). DFT-MD simulations were performed using CP2K [12]. NPT simulations were run at a temperature of 300 K and pressure of 1 atm for 10 ps, using the revised Perdue-Burke-Ernzerhof (revPBE) functional with double zeta valence polarized (DZVP) basis set and Grimme-D2 pair potential for van der Waals interactions. A vacuum layer of 10 Å in the z-direction was used to reduce the effects of periodic boundary conditions on the system.

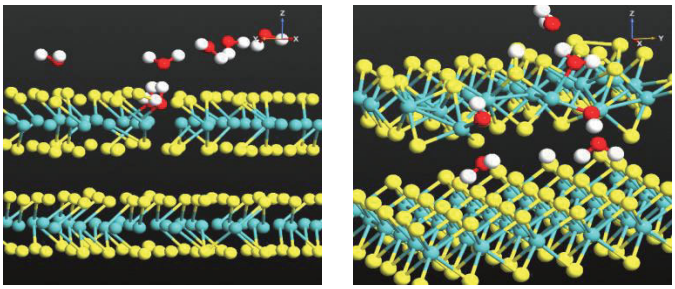

a) b)

Fig. 7: Absorption of H_2O at a MoS_2 bilayer: OH adsorption at (a) a grain boundary and (b) the edge sites exposed to water.

Water is observed to dissociate, with hydroxide molecules being absorbed at exposed Mo and H at nearby S atoms (Fig. 7a). Similar behavior was observed at the edges exposed to water (Fig. 7b). These observations correlate well with previously observed models of water-gas–shift reactions near MoS_2 edges [4].

The oxidation at edge sites was also studied using DFT-MD in similar fashion to water absorption. Fig. 8a shows the starting configuration of the simulations while Fig. 8b shows the configuration after 10ps. O_2 is observed to bond as a molecular group in many cases but also as single atom, which is observed to bond to edge Mo. As in the case of water, Mo is observed to attract O.

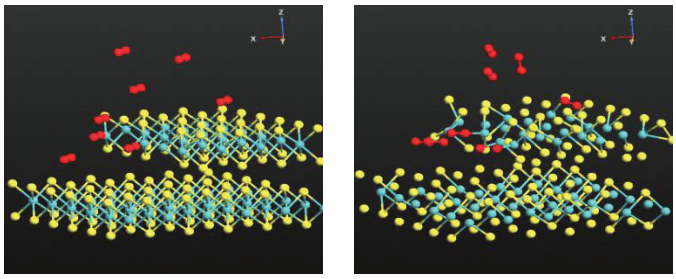

a) b)

Fig. 8: Absorption of O_2 at a MoS_2 bilayer: O_2 adsorption at a MoS_2 edge in ta) the initial configuration and (b) after 10 ps of DFT-MD simulation.

CONCLUSIONS

A combination of methods was used to study the effect of structural defects – in this case, atomic vacancies – on the electrical properties of MoS_2 bilayers. The absence of either S or Mo atoms leads to the formation of gap states that, in the case of single vacancy and particularly in the case of Mo vacancy, create a significant current at low voltages. Single S vacancies lead to no significant change in the conduction paths for electrons or holes; however, Mo vacancies completely disrupt electron transport without seriously affecting hole transport. The opposite is found for the double S vacancy, where hole transport is eliminated but electron transport is not affected. DFT-MD simulations provided some insight on how moisture and oxidation affect the device, information that is being used to study transport in these devices in the presence of humidity and oxidation.

REFERENCES

[1] S. Butler, S. Hollen, L. Cao, Y. Cui, J. Gupta, H. Gutie, T. Heinz, S. Hong, J. Huang, A. Ismach, E. Johnston-Halperin, M. Kuno, V. Plashnitsa, R. Robinson, R. Ruoff, S. Salahuddin, J. Shan, L. Shi, O. Spencer, M. Terrones, W. Windl, and J. Goldberger, "Progress, Challenges, Opportunities in Two-Dimensional Materials Beyond Graphene," ACS Nano, vol. 7, pp. 2898–2926, April 2013.

[2] S. Tongay, J. Zhou, C. Ataca, J. Liu, J.Kang, T.Matthews, L. You, J. Li, J. Grossman, and J. Wu, "Broad-range modulation of light emission in two-dimensional semiconductors by molecular physisorption gating." Nano Lett., vol. 13, pp. 2831–2836, June 2013.

[3] F. Zhang and J. Appenzeller, "Tunability of Short-Channel Effects in MoS2 Field-Effect Devices," Nano Lett., vol. 15, pp. 301–306, January 2015.

[4] Z. Zhang, X. Zou, V. H. Crespi, and B. I. Yakobson, "Intrinsic magnetism of grain boundaries in two-dimensional metal dichalcogenides," ACS Nano, vol. 7, pp. 10475–10481, December 2013.

[5] X.-R. Shi, S.-G. Wang, J. Hu, H. Wang, Y.-Y. Chen, Z. Qin, and J. Wang, "Density functional theory study on water–gas-shift reaction over molybdenum disulfide," Appl. Catal. A, vol. 365, pp. 62–70, August 2009.

[6] S. Ida and T. Ishihara. "Recent Progress in Two-Dimensional Oxide Photocatalists for Water Splitting" J. Phys. Chem. Lett., vol. 5, p. 2533-2542, August 2014.

[7] Y. Chang, R. Nikam, C. Lin, J. Huang, C. Tseng, C. Hsu, C. Cheng, C. Su, L. Li, and D. Chua. "Enhanced Electrocatalytic Activity of MoSx on TCNQ-Treated Electrode for Hydrogen Evolution Reaction" ACS Appl. Mater. Inter, vol. 6, p. 17679-17685, October 2014.

[8] C. Muratore, V. Varshney, J. J. Gengler, J. J. Hu, J. E. Bultman, T. M. Smith, P. J. Shamberger, B. Qiu, X. Ruan, a. K. Roy, and a. a. Voevodin, "Cross-plane thermal properties of transition metal dichalcogenides," Appl. Phys. Lett., vol. 102, p. 081604, February 2013.

[9] Atomistix ToolKit version 2014.2, QuantumWise A/S (www.quantumwise.com)

[10] S. Datta, "Electronic Transport in Mesoscopic Systems", Cambridge University Press, Cambridge, UK, 1995.

[11] W. Zhou, X. Zou, S. Najmaei, Z. Liu, Y. Shi, J. Kong, J. Lou, P. M. Ajayan, B. I. Yakobson, and J.-C. Idrobo, "Intrinsic structural defects in monolayer molybdenum disulfide," Nano Lett., vol. 13, no. 6, pp. 2615–2622, June 2013.

[12] CP2K-Open source molecular dynamics, http://www.cp2k.org